ON THE EFFECTIVENESS OF FEATURE-BASED LIDAR POINT CLOUD REGISTRATION

J.J. Jaw [a, *], T.Y. Chuang [a]

[a] Department of Civil Engineering, National Taiwan University, 1, Roosevelt Rd., Sec. 4, Taipei 10617, Taiwan – (jejaw,d95521008)@ntu.edu.tw

Commission III, WG III/2

KEY WORDS: Feature-based, LIDAR, Registration, 3-D similarity transformation model

ABSTRACT:

LIDAR systems have been regarded as novel technologies for efficiently acquiring 3-D geo-spatial information, resulting in broad applications in engineering and management fields. Registration of LIDAR point clouds of consecutive scans or different platforms is a prerequisite for fully exploiting advantages of afore-mentioned applications. In this study, the authors integrate point, line and plane features, commonly seen geometric primitives and readily detected or derived from point clouds, for establishing a multi-feature 3-D similarity transformation model, both functional and stochastic, and illustrate the feasibility of the proposed methodologies on the effectiveness of employed features through theoretical identifications and experimental demonstrations.

1. INTRODUCTION

Registration of LIDAR point clouds of consecutive scans or different platforms is a prerequisite for fully exploiting advantages of afore-mentioned applications. Based on how the registrations are established, dispersed point basis and feature basis can be identified as two main distinctions in this regard. Dispersed point, ICP (Besl and McKay, 1992) algorithm for example, can be utilized to estimate the transformation parameters without involving actual feature extraction, while requiring high quality of parameter's approximation. On the other hand, feature-based approach relies on distinct features and transformation parameters are to be solved based on feature correspondence.

Points, lines and planes are three most common as well as essential geometric features used to perform the point cloud transformation. They are especially abundant in urban areas with man-made structures. Studies on how to establish the mathematic model and solve transformation parameters by geometric features have been seen in literature as follows. Stamos and Allen (2002) illustrated partial task for range-to-range registration where conjugate 3-D line features for solving the transformation parameters between scans were manually corresponded. Stamos and Leordeanu (2003) developed an automated registration algorithm where pair-wise registration strategy with the additional information of the supporting planes on which the 3-D lines lie facilitated the match. Habib *et al*. (2005) utilized straight-line segments for registering LIDAR data sets and photogrammetric data sets though. Gruen and Akca (2005) developed the least-squares approach tackling surface and curve matching. Besides, Akca (2003) designed target or landmarks that can be easily identified from point clouds are well served for point cloud registration. Rabbani *et al*. (2007) proposed a framework for pair-wise registration of shapes represented by point cloud data, based on the assumption that the points are sampled from a surface and the problem of aligning two point clouds can be formulated as a minimization of the squared distance between the underlying surfaces. von Hansen (2007) presented a plane-based approach that the point clouds are first split into a regular raster and made a gradual

progress for automatic registration. von Hansen *et al.*(2008) proposed estimating transformation parameters between terrestrial and aerial LIDAR point clouds on line feature basis. Jaw and Chuang (2008) conducted the registration of ground-based LIDAR point clouds by means of 3-D line features simultaneously in a complete procedure.

However, the transformation parameters are usually solved by single type of feature among all choices of proposed methodology. When facing with the problems, such as obstruction of corresponding pairs, weak geometric strength of transformation, lack of measurements, weak overlapping and so forth, the negative effects upon the registration quality would be obvious. In consideration with that, a multi-feature transformation model applying to registration can offer more flexibility and more reliability in the face of diversified LIDAR point clouds. In this paper, the authors present the functional and stochastic model which employs point, line, and plane features as a mean for conducting the registration. Each kind of feature can be exclusively used or combined depending on the scene geometry. Hence the unreliable effects caused by the discrepancy mentioned above can be restrained, and the high degree of working flexibility and highly accurate results are more likely to be met. To the authors' knowledge, few studies tackle the registration scheme basing on various geo-features. Therefore, this study demonstrates the effectiveness of employing multi-features with implementing both functional and stochastic models solving for transformation parameters of registering LIDAR point clouds.

2. METHODOLOGY

The proposed multi-feature transformation model consists of point-based, line-based, and plane-based 3-D similarity transformations. Seven parameters including a scale parameter (S), a translation vector ($\mathcal{T}[T_X, T_Y, T_Z]^T$), and a rotation matrix ($\mathcal{R}\{\omega, \varphi, \kappa\}$) are considered for the transformation. Considering that 3-D line feature and plane patch can be symbolized by manifold forms, two end-points of a line segment, $\mathcal{L}\{X_{(1)i}, Y_{(1)i}, Z_{(1)i}, X_{(2)i}, Y_{(2)i}, Z_{(2)i}\}$, the six-parameter form of $\mathcal{L}\{l_i, m_i, n_i, X_{0i}, Y_{0i}, Z_{0i}\}$ or the four-parameter representation of

---

$\mathcal{L}\{d_i, e_i, 1, p_i, q_i, 0\}$ are alternatively employed when presenting 3-D line features (Roberts, 1988; Strunz, 1993). As for 3-D plane patch, three-parameter $\mathcal{P}\{\theta_i, \varphi_i, \rho_i\}$ or $\mathcal{P}\{a_i, b_i, c_i\}$ can be chosen to form plane equations. High flexibility of presenting features is one of the advantages firstly identified in this work. The mathematical formulas proposed in this study are specified in detail as follows.

2.1 Multi-feature Integration Transformation model

Multi-feature transformation model is established by integrating the point, line and plane transformation models solving for the seven parameters. None of any specific geometric features is imperative as long as the condition of solving parameters is fulfilled. It turns out that the multi-feature integration scheme can offer higher degree of flexibility and higher accuracy to fulfil the LIDAR point cloud registration tasks in an optimal way. At the methodological level, the spatial transformation of point clouds can be established by the correspondence between conjugate points, or by the co-trajectory relation of conjugate lines, or by the corresponding parameters of conjugate planes. The point-based formula is shown as Eq. (1) which is the fundamental similarity transformation based on point-to-point correspondence. To balance the transformation equation for solving seven parameters while providing a sufficient datum, three non-collinear points are at least needed for a non-singular solution. The point-based equation can be applied to formulating line-based transformation as illustrated in next paragraph.

$$\begin{bmatrix} X_{(2)i} \\ Y_{(2)i} \\ Z_{(2)i} \end{bmatrix} = \begin{bmatrix} T_X \\ T_Y \\ T_Z \end{bmatrix} + S \begin{bmatrix} m_{11} & m_{12} & m_{13} \\ m_{21} & m_{22} & m_{23} \\ m_{31} & m_{32} & m_{33} \end{bmatrix} \begin{bmatrix} X_{(1)i} \\ Y_{(1)i} \\ Z_{(1)i} \end{bmatrix} \quad (1)$$

where $m_{11} = cos(\kappa)\,cos(\varphi)$; $m_{12} = sin(\kappa)\,cos(\omega) + cos(\kappa)\,sin(\varphi)\,sin(\omega)$;
$m_{21} = -sin(\kappa)\,cos(\varphi)$;
$m_{13} = sin(\kappa)\,sin(\omega) - cos(\kappa)\,sin(\varphi)\,cos(\omega)$;
$m_{32} = -cos(\varphi)\,sin(\omega)$;
$m_{22} = cos(\kappa)\,cos(\omega) - sin(\kappa)\,sin(\varphi)\,sin(\omega)$;
$m_{33} = cos(\varphi)\,cos(\omega)$;
$m_{23} = cos(\kappa)\,sin(\omega) + sin(\kappa)\,sin(\varphi)\,cos(\omega)$;
$m_{31} = sin(\varphi)$; $\omega 、 \varphi 、 \kappa$: the rotation angle with respect to X, Y, Z axis;
i: the ith point feature, $i = 1, 2, 3 \cdots n_{Pt}$;
n_{Pt}: the number of conjugate points;
$(X_{(1)i}, Y_{(1)i}, Z_{(1)i})$: the ith point in coordinate system 1;
$(X_{(2)i}, Y_{(2)i}, Z_{(2)i})$: the ith point in coordinate system 2;

2.1.1 Line-based Transformation Model: The line-based transformation model proposed in this study can be analyzed by two forms. The condition for transformation model based on two end-points of line segment is realized by constraining that each 3-D end-point of line feature transformed to another coordinate system should be collinear with its conjugate counterpart, implying that the point to point correspondence is not needed. That is, the collinear property for one end-point can be established by Eq. (2).

$$\begin{cases} m_{(2)i}\left(X_{(2)i} - X_{(1')i}\right) - l_{(2)i}(Y_{(2)i} - Y_{(1')i}) = 0 \\ n_{(2)i}\left(Y_{(2)i} - Y_{(1')i}\right) - m_{(2)i}(Z_{(2)i} - Z_{(1')i}) = 0 \end{cases} \quad (2)$$

where i: the ith line feature, $i = 1, 2, 3 \cdots n_L$;
n_L: the number of conjugate line pairs;
$(l_{(2)i}, m_{(2)i}, n_{(2)i})$: the directional vector of ith line in coordinate system 2;
$(X_{(1')i}, Y_{(1')i}, Z_{(1')i})$: the end-point $(X_{(1)i}, Y_{(1)i}, Z_{(1)i})$ of ith line transformed by Eq. (1) from coordinate system 1 to system 2;
$(X_{(2)i}, Y_{(2)i}, Z_{(2)i})$: the end-point of ith conjugate line in coordinate system 2;

As revealed in Eq. (2), one 3-D line correspondence contributes four equations (two for each end-point). There must be at least two non-coplanar 3-D line pairs in order to solve the transformation parameters. More detail about the line-based 3-D similarity transformation can be referred to (Jaw and Chuang, 2008). In the similar way, the condition for transformation model based on four parameters can also be realized by constraining that the directional vector and the punctured-point of 3-D line features transformed to another coordinate system should be collinear with their conjugate correspondents. The four independent parameters of 3-D line can be derived from the six-parameter set as shown in Eq. (3). Therefore, the mathematical formula can be established as Eq. (4), in which the transformation of directional vector is shown as Eq. (5).

$$\begin{bmatrix} X_i \\ Y_i \\ Z_i \end{bmatrix} = \begin{bmatrix} X_{0i} \\ Y_{0i} \\ Z_{0i} \end{bmatrix} + t_i \begin{bmatrix} l_i \\ m_i \\ n_i \end{bmatrix} = \begin{bmatrix} p_i \\ q_i \\ 0 \end{bmatrix} + z_i \begin{bmatrix} d_i \\ e_i \\ 1 \end{bmatrix} \quad (3)$$

where $[X_{0i} \quad Y_{0i} \quad Z_{0i}]^T$: the initial point of ith line;
$[l_i \quad m_i \quad n_i]^T$: the directional vector of ith line;
$[p_i \quad q_i \quad 0]^T$: the punctured-point of ith line based on X-Y plane;
$[d_i \quad e_i \quad 1]^T$: the reductive directional vector of ith line based on X-Y plane;
$t_i 、 z_i$: constants

$$\begin{cases} m_{(2)i}(X_{0(2)i} - X_{0(1')i}) - l_{(2)i}(Y_{0(2)i} - Y_{0(1')i}) = 0 \\ n_{(2)i}(Y_{0(2)i} - Y_{0(1')i}) - m_{(2)i}(Z_{0(2)i} - Z_{0(1')i}) = 0 \\ m_{(2)i} \cdot l_{(1')i} - l_{(2)i} \cdot m_{(1')i} = 0 \\ n_{(2)i} \cdot m_{(1')i} - m_{(2)i} \cdot n_{(1')i} = 0 \end{cases} \quad (4)$$

where $(X_{0(1')i}, Y_{0(1')i}, Z_{0(1')i})$: the puncture point $(X_{0(1)i}, Y_{0(1)i}, Z_{0(1)i})$ of ith line transformed by Eq. (1) from coordinate system 1 to system 2;
$(X_{0(2)i}, Y_{0(2)i}, Z_{0(2)i})$: the punctured point of ith conjugate line in coordinate system 2;
$[l_{(1')i}, m_{(1')i}, n_{(1')i}]^T$: the directional vector $[l_{(1)i}, m_{(1)i}, n_{(1)i}]^T$ of ith line transformed by Eq. (5) from coordinate system 1 to system 2;

$$\begin{bmatrix} l_{(1')i} \\ m_{(1')i} \\ n_{(1')i} \end{bmatrix} = \begin{bmatrix} m_{11} & m_{12} & m_{13} \\ m_{21} & m_{22} & m_{23} \\ m_{31} & m_{32} & m_{33} \end{bmatrix} \cdot \begin{bmatrix} l_{(1)i} \\ m_{(1)i} \\ n_{(1)i} \end{bmatrix} \quad (5)$$

Note that the six variables in Eq. (4) would alter as considering different reference planes. Similarly, the conjugate lines on

different coordinate systems may have varied reference planes. The appropriate usages of parameters can be referred to Table 1 according to the associated situations.

Reference plane	Observation	Constant
X-Y	$X_{0i} = p_i$ 、 $Y_{0i} = q_i$ 、 $l_i = d_i$ 、 $m_i = e_i$	$Z_{0i} = 0$ 、 $n_i = 1$
Y-Z	$Y_{0i} = q_i$ 、 $Z_{0i} = r_i$ 、 $m_i = e_i$ 、 $n_i = f_i$	$X_{0i} = 0$ 、 $l_i = 1$
X-Z	$X_{0i} = p_i$ 、 $Z_{0i} = r_i$ 、 $l_i = d_i$ 、 $n_i = f_i$	$Y_{0i} = 0$ 、 $m_i = 1$

Table 1. The associated variables of reference planes

2.1.2 Plane-based Transformation Model: A special 3-D plane can be formulated by three elements of a normal vector in Cartesian coordinate system, or by two angles and one length to describe the normal vector in a spherical coordinate system. In this work, the transformation functions are adapted to both formulas. The first one, shown in Eq. (6), presents the plane equation with three elements of normal vector. As a consequence of mathematical derivation, the transformation of normal vector can be established as Eq. (7). Then, depending on the constraints of angle and distance, the transformation model based on $\{a_i, b_i, c_i\}$ is shown as Eq. (8).

$$a_i X + b_i Y + c_i Z + 1 = 0 \tag{6}$$

$$\begin{cases} a_{(1')i} = \\ a_{(1)i}m_{11} + b_{(1)i}m_{12} + c_{(1)i}m_{13}/(S - a_{(1)i}m_{41} - b_{(1)i}m_{42} - c_{(1)i}m_{43}) \\ b_{(1')i} = \\ a_{(1)i}m_{21} + b_{(1)i}m_{22} + c_{(1)i}m_{23}/(S - a_{(1)i}m_{41} - b_{(1)i}m_{42} - c_{(1)i}m_{43}) \\ c_{(1')i} = \\ a_{(1)i}m_{31} + b_{(1)i}m_{32} + c_{(1)i}m_{33}/(S - a_{(1)i}m_{41} - b_{(1)i}m_{42} - c_{(1)i}m_{43}) \end{cases} \tag{7}$$

$$\begin{cases} a_{(2)i}a_{(1')i} + b_{(2)i}b_{(1')i} + c_{(2)i}c_{(1')i} - \\ \sqrt{(a_{(2)i})^2 + (b_{(2)i})^2 + (c_{(2)i})^2}\sqrt{(a_{(1')i})^2 + (b_{(1')i})^2 + (c_{(1')i})^2} = 0 \\ \sqrt{(a_{(2)i})^2 + (b_{(2)i})^2 + (c_{(2)i})^2} - \sqrt{(a_{(1')i})^2 + (b_{(1')i})^2 + (c_{(1')i})^2} = 0 \end{cases} \tag{8}$$

where $m_{41} = m_{11}T_X + m_{21}T_Y + m_{31}T_Z$;
$m_{42} = m_{12}T_X + m_{22}T_Y + m_{32}T_Z$;
$m_{43} = m_{13}T_X + m_{23}T_Y + m_{33}T_Z$;
i: the ith plane feature, $i = 1, 2, 3 \cdots n_{PL}$;
n_{PL}: the number of conjugate plane pairs;
$(a_{(1)i}, b_{(1)i}, c_{(1)i})$: the normal vector $(a_{(1)i}, b_{(1)i}, c_{(1)i})$ of ith plane transferred from coordinate system 1 to system 2;
$(a_{(2)i}, b_{(2)i}, c_{(2)i})$: the normal vector of ith plane in coordinate system 2;

The second type of a 3-D plane can be formulated as Eq. (9) where the three parameters $(\theta_i, \varphi_i, \rho_i)$ define a vector from the original to the nearest point on the plane. As a consequence of mathematical derivation, the correspondence of the three plane parameters can be expressed as Eq. (10) and served as a transformation model.

$$sin\theta_i cos\varphi_i X + sin\theta_i sin\varphi_i Y + cos\theta_i Z = \rho_i \tag{9}$$

where θ_i: the angle between z-axis and the vector;
φ_i: the angle between x-axis and the projection of the vector onto X-Y plane;
ρ_i: the perpendicular distance from the original to the plane;

$$\begin{cases} F_1/F_2 - tan\theta_{(2)i}(sin\varphi_{(2)i} + cos\varphi_{(2)i}) = 0 \\ F_3 - S \cdot \rho_{(1)i} + \rho_{(2)i} = 0 \end{cases} \tag{10}$$

where $(\theta_{(1)i}, \varphi_{(1)i}, \rho_{(1)i})$: the normal vector of ith plane in coordinate system 1;
$(\theta_{(2)i}, \varphi_{(2)i}, \rho_{(2)i})$: the normal vector of ith plane in coordinate system 2;
$F_1 = (m_{11} + m_{21})sin\theta_{(1)i}cos\varphi_{(1)i} + (m_{12} + m_{22})sin\theta_{(1)i}sin\varphi_{(1)i} + (m_{13} + m_{23})cos\theta_{(1)i}$;
$F_2 = m_{31}sin\theta_{(1)i}cos\varphi_{(1)i} + m_{32}sin\theta_{(1)i}sin\varphi_{(1)i} + m_{33}cos\theta_{(1)i}$;
$F_3 = -m_{41}sin\theta_{(1)i}cos\varphi_{(1)i} - m_{42}sin\theta_{(1)i}sin\varphi_{(1)i} - m_{43}cos\theta_{(1)i}$;

Thus, basing on Eq. (8) and Eq. (10), one pair of matched planes can contribute two equations; four independent and well distributed planes are minimally required for a stable solution. The configurations of the transformation models of these three types of features mentioned above are summarized in Table 2. Note that in Table 2 and Table 3, the numbers of conjugate features for point, line and planes are notated by n_{Pt}, n_L and n_{PL}, respectively, while n_s is the number of scans.

	Num. of Eq.	Min. Num. of Meas.	Redundancy	Min. Num. of Meas. ($n_s = 2$)
Point-based model	$3n_{Pt}$	$n_{Pt} \geq 7(n_s - 1)/3$	$3n_{Pt} - 7(n_s - 1)$	3
Line-based model	$4n_L$	$n_L \geq 7(n_s - 1)/4$	$4n_L - 7(n_s - 1)$	2
Plane-based model	$2n_{PL}$	$n_{PL} \geq (n_s - 1) \times 4$	$2n_{PL} - 7(n_s - 1)$	4

Table 2. The configurations of the transformation models

2.1.3 Adjustment Model for Multi-feature Integration: In this study, the unknown parameters of multi-feature transformation are estimated by virtue of the general model of least-squares adjustment. The descriptions of the mathematical function dealing with two scans are given as Eq. (11), and the related symbols are explained in Table 3.

$$w_{p_1 \times 1} = A_{p_1 \times 7} \xi_{7 \times 1} + B_{p_1 \times p_2}(y_{p_2 \times 1} + e) \; , e \sim (0, \textstyle\sum = \sigma_0^2 P^{-1}) \tag{11}$$

where y: observation vector;
e: error vector;
P: weight matrix;
ξ: incremental parameter vector;
σ_0^2: variance component;
w: discrepancy vector;

	A	B	p_1	p_2
Multi-feature model	partial derivative coefficient matrix of Eq. (1), (2), (4), (8) or (10) with respect to parameters	partial derivative coefficient matrix of Eq. (1), (2), (4), (8) or (10) with respect to observations	$(3n_{Pt} + 4n_L + 2n_{PL})$	$(6n_{Pt} + 8n_L + 6n_{PL})$ or $(6n_{Pt} + 12n_L + 6n_{PL})$

Table 3. The definitions of symbols

2.2 The Effectiveness of Multi-features

The measurements can be generally made up of all available and qualified features. However, the constraint power varies with different types of features. Point-based transformation is constituted on the point-to-point constraint with a strongest strength. Line-based transformation is established by means of the co-trajectory constraint leaving degrees of freedom of a scale, a translation, and a rotation along the line for each line feature observation. Similarly, a plane feature results in a scale, a rotation and two translation parameters on this plane ambiguous.

On the other hand, point features in LIDAR point clouds are usually so lurked that they need to be extracted through the intersection of plane or line features. Point clouds nearby physical edges are likely to be distorted because of uneven geometric information when analyzing waveforms of their footprints. Therefore, it seems to pose that none of the single feature usage would bring about satisfactory registration result, suggesting that the combination of multi-features would support the balance between constraint power, availability, and accuracy of employed features. The beneficial registered results made by qualified features and the effectiveness of registration performed by each kind of and combined geo-features are analyzed by the following experiments.

3. EXPERIMENTS AND ANALYSES

For validating the ability of geometric constraints and the effectiveness upon the registration accuracy afforded by each individual feature and combined features, the following experiments by means of simulated data were designed.

3.1 The Data Configuration and Transformation

The simulated data of point clouds and the location of features are illustrated in Figure 1 where the 8 blue dots at corners, the 12 res lines and the small dots with different colors present point, line and plane features, respectively. The above simulated point cloud was then transformed by a set of transformation parameter serving as a data scanned in next station. All point clouds were contaminated with a noise of zero mean and 0.015-m standard deviation (about ±0.0088m in each coordinate component). In this configuration, each kind of feature has

pretty even distribution. Moreover, the origin of working coordinate system has been moved to the centroid of the point cloud for concerning numerical stability. Then, the transformation parameters were estimated considering employing different geo-features, points (directly chosen from point cloud), lines (directly chosen from point cloud), intersected points, interested lines, fitted planes and all combined intersected and fitted features. And the registration accuracies were evaluated by 400 regularly distributed check points. Note that Eq. (2) and Eq. (10) for line and plane feature, respectively, were adopted in this test.
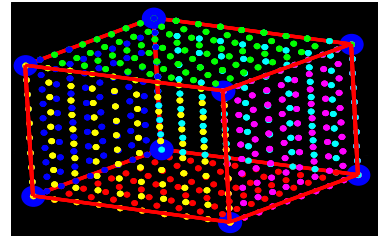
Figure 1. The illustration of experiment field

3.2 The Results and Analyses

Points and lines as indicated in Table 4 and Table 5 were directly chosen out of point clouds, thus their positioning errors were considered the same as point cloud itself. On the other hand, the standard deviations of the intersected points, the intersected lines and the fitted planes must be estimated based on the error propagation of occuring intersection. The results of the estimated transformation parameters together with their stansard deviations and the registration accuracies for employing different types of features are listed in Table 4 and Table 5.

Table 5 presents, starting from 3rd row and 2nd column, accuracies of check points for both RMSE (root mean square error) and standard deviation (denoted as sigma_, an average of standard deviations at each component) through error propagation. The former one may be regarded as an empirical accuracy, while the latter one, a theoretical accuracy. When the check points were of true values, the accuracy suggests only the

quality of transformation parameters. And when the check points were noised with the same error as point clouds, the accuracy in Table 5 reflects the quality of the registration on point clouds. From Table 4 and Table 5, one can easily see that when using intersected features (points or lines extracted by intersecting planes) and fitted planes, a better parameter as well as registration accuracy can be obtained than when applying

directly measured features. As for the registration discrepancies among modes of different intersected or fitted features are not truly significant, implying almost equivalent contribution to the registration quality, two planes versus their intersected line, three planes versus their intersected point, just to name a few. Above all, combining all intersected and fitted features brings about the best registration quality.

True values / Feature type	S	ω (rad)	φ (rad)	κ (rad)	T_X (m)	T_Y (m)	T_Z (m)
	1.5	0.2	0.3	0.4	5	6	2
Point	1.5007±0.0004	0.2997±0.0003	0.2005±0.0003	0.4996±0.0004	4.9975±0.0032	5.9951±0.0034	2.0005±0.0022
Line	1.5003±0.0005	0.2995±0.0005	0.2005±0.0005	0.5006±0.0004	5.0075±0.0043	6.0058±0.0038	1.9944±0.0048
Intersected Point	1.5000±0.0002	0.2999±0.0002	0.1996±0.0002	0.5001±0.0002	4.9991±0.0016	6.0024±0.0017	2.0015±0.0016
Intersected Line	1.4999±0.0001	0.2998±0.0001	0.1996±0.0001	0.5001±0.0001	4.9991±0.0011	6.0023±0.0010	2.0015±0.0012
Fitted Plane	1.4999±0.0002	0.3001±0.0002	0.1997±0.0003	0.4998±0.0003	5.0006±0.0014	6.0029±0.0016	2.0009±0.0019
Combined feature	1.5000±0.0001	0.2999±0.0001	0.1998±0.0001	0.5001±0.0001	4.9993±0.0008	6.0026±0.0009	2.0013±0.0009

Table 4. The result of transformation parameters

Feature type	Accuracy of Check point	RMSE_X	RMSE_Y	RMSE_Z	RMSE_Total	Sigma_X	Sigma_Y	Sigma_Z	Dist.
Point	±0	0.0036	0.0055	0.0028	0.0071	0.0039	0.0039	0.0029	0.0063
	±0.015	0.0162	0.0161	0.0148	0.0273	0.0156	0.0166	0.0164	0.0281
Line	±0	0.0086	0.0063	0.0066	0.0125	0.0051	0.0047	0.0056	0.0090
	±0.015	0.0179	0.0160	0.0153	0.0285	0.0140	0.0138	0.0142	0.0242
Intersected Point	±0	0.0015	0.0025	0.0021	0.0035	0.0019	0.0020	0.0020	0.0034
	±0.015	0.0160	0.0150	0.0149	0.0265	0.0137	0.0139	0.0138	0.0239
Intersected Line	±0	0.0014	0.0024	0.0023	0.0037	0.0023	0.0022	0.0014	0.0033
	±0.015	0.0160	0.0150	0.0149	0.0265	0.0133	0.0133	0.0134	0.0231
Fitted Plane	±0	0.0014	0.0030	0.0016	0.0037	0.0021	0.0022	0.0025	0.0040
	±0.015	0.0159	0.0151	0.0149	0.0265	0.0139	0.0156	0.0143	0.0253
Combined feature	±0	0.0017	0.0026	0.0011	0.0033	0.0015	0.0015	0.0015	0.0026
	±0.015	0.0159	0.0150	0.0148	0.0265	0.0131	0.0131	0.0131	0.0226

P.S. RMSE_Total $= \sqrt{(RMSE\_X)^2 + (RMSE\_Y)^2 + (RMSE\_Z)^2}$; Dist. $= \sqrt{(Sigma\_X)^2 + (Sigma\_Y)^2 + (Sigma\_Z)^2}$

Table 5. The result of registration accuracy (unit: meter)

4. CONCLUSIONS

Natural and man-made scenes are usually complex and versatile. The proposed multi-feature integration combining point, line, and plane features seems so potential for reaching an optimal registration and can be considered as a more reliable and flexible approach to dealing with situations when lacking correspondents against scene geometry. The contributions concluded in this paper are the discussion of the ability of geometric constraints and the verification of the effectiveness among point, line and plane features with a quantification analysis. The quantitative as well as qualitative analyses verified through the experiments would offer a valuable reference to effectively and efficiently working on the mission of LIDAR point cloud registration.

5. REFERENCES

Akca, D., 2003. Full Automatic Registration of Laser Scanner Point Clouds, *Optical 3D Measurement Techniques VI*, pp. 330-337.

Gruen, A., and Akca, D., 2005. Least squares 3D surface and curve matching, *ISPRS Journal of Photogrammetry and Remote Sensing*, 59(3), pp. 151-174.

Habib, A., Mwafag, G., Michel, M., and Al-Ruzouq, R., 2005. Photogrammetric and LIDAR Data Registration Using Linear Features, *Photogrammetric Engineering & Remote Sensing*, 71(6), pp. 699–707.

Jaw, J.J., and T.Y. Chuang, 2008. Registration of LIDAR Point Clouds by means of 3D Line Features, *JCIE Journal of the Chinese Institute of Engineers*, 31(6), pp. 1031-1045.

Roberts, K.S., 1988. A new representation for lines. *IEEE Proceedings of Computer Vision and Pattern recognition*, pp. 635–640.

Rabbani T., S. Dijkman, F. Heuvel, and G. Vosselman, 2007. An Integrated Approach for Modelling and Global Registration of Point Clouds, *ISPRS journal of Photogrammetry and Remote Sensing*, 61, pp. 355-370.

Strunz, G., 1993. *Bildorientierung und Objektrekonstruktion mit Punkten, Linien und Flächen*, Dissertation, Deutsche Geodätische Kommission, Verlag der Bayerischen Akademie der Wissenschatten,München, 95p.

Stamos, I., and Allen, P.K., 2002. Geometry and Texture Recovery of Scenes of Large Scale, *Computer Vision and Image Understanding*, 88(2), pp. 94-118.

Stamos, I., and Leordeanu, M., 2003. Automated Feature-based Range Registration of Urban Scenes of Large Scale,

Proceedings of IEEE Computer Society Conference on Computer Vision and Pattern Recognition, 2, pp. 555-561.

von Hansen, W., 2007. Registration of Agia Sanmarina LIDAR Data Using Surface Elements, *IAPRS* 36(Part 3/W49A), pp. 93-97.

von Hansen, W., Gross, H., and Thoennessen, U., 2008. Line-based Registration of Terrestrial and Aerial LIDAR Data, *ISPRS proceeding*, 37(B3a), pp. 161-166.